RADIATION RESEARCH **164**, 180–193 (2005)
0033-7587/05 $15.00


# Monte Carlo Simulation of Base and Nucleotide Excision Repair of Clustered DNA Damage Sites. I. Model Properties and Predicted Trends

V. A. Semenenko,[a] R. D. Stewart[a,1] and E. J. Ackerman[b]

[a] *Purdue University, School of Health Sciences, West Lafayette, Indiana 47907-2051; and* [b] *Pacific Northwest National Laboratory, Richland, Washington 99352-0999*

**Semenenko, V. A., Stewart, R. D. and Ackerman, E. J. Monte Carlo Simulation of Base and Nucleotide Excision Repair of Clustered DNA Damage Sites. I. Model Properties and Predicted Trends.** ***Radiat. Res.*** **164, 180–193 (2005).**

**DNA is constantly damaged through endogenous processes and by exogenous agents, such as ionizing radiation. Base excision repair (BER) and nucleotide excision repair (NER) help maintain the stability of the genome by removing many different types of DNA damage. We present a Monte Carlo excision repair (MCER) model that simulates key steps in the short-patch and long-patch BER pathways and the NER pathway. The repair of both single and clustered damages, except double-strand breaks (DSBs), is simulated in the MCER model. Output from the model includes estimates of the probability that a cluster is repaired correctly, the fraction of the clusters converted into DSBs through the action of excision repair enzymes, the fraction of the clusters repaired with mutations, and the expected number of repair cycles needed to completely remove a clustered damage site. The quantitative implications of alternative hypotheses regarding the postulated repair mechanisms are investigated through a series of parameter sensitivity studies. These sensitivity studies are also used to help define the putative repair characteristics of clustered damage sites other than DSBs.** 

## INTRODUCTION

Exposure to ionizing radiation produces many different types of DNA damage, including damaged bases and strand breaks (*1*). Although similar types of DNA lesions are produced by endogenous processes and various physical and chemical agents (*2*), the relative yield and spatial arrangement of damaged nucleotides can be quite different. Groups of several damaged nucleotides within one or two helical turns of the DNA, often referred to as multiply damaged sites (*1*) or clustered damages (*3*), are known to be a hallmark of ionizing radiation. Theoretical considerations suggest that, in addition to isolated lesions, low-LET radiation can create clusters with as many as 10 lesions (*4*). High-LET radiation is capable of producing damage of even greater complexity, i.e. up to 25 lesions per cluster (*4*). Endogenous processes mainly produce isolated lesions, although clustered damage sites may be formed in cells that are deficient in DNA repair (*5*).

One form of radiation-induced clustered damage that is readily observed experimentally is the double-strand break (DSB). The production of other, non-DSB types of clustered damage has been documented for radiation of different quality in a variety of biological systems (*6–13*). These studies show that DSBs comprise only 20–30% of the total yield of clustered damage sites (*8–12*). Although DSBs are widely viewed as the most critical form of DNA damage produced by ionizing radiation, other types of clustered damage have long been hypothesized to make a substantial contribution to radiation-induced cell killing and mutagenesis (*14, 15*). The underlying hypothesis is that clustered damage is hard to repair because repair enzymes may not always have an intact template to guide the replacement of damaged nucleotides (*1*). Studies with wild-type and repair-deficient bacteria provide direct support for the hypothesis that some types of clustered damage have greater mutagenic potential than isolated DNA lesions (*16, 17*). Experiments also show that the repair of clustered damages can result in the formation of potentially lethal DSBs (*18, 19*).

Many different types of oxidative DNA damage, ranging from modified bases to AP (apurinic/apyrimidinic) sites to strand breaks, are repaired by base excision repair (BER). Two modes of the BER process have been observed in both prokaryotes (*20*) and eukaryotes (*21–23*). The excision and replacement of a single nucleotide, termed short-patch base excision repair (SP BER), occurs in most cases (*24*). The other mode, long-patch base excision repair (LP BER), results in the removal of fragments 2–13 nucleotides long (*25*).

Nucleotide excision repair (NER) is an enzymatically distinct DNA repair pathway. In eukaryotes, oligonucleotide fragments approximately 24–32 nucleotides in length are replaced during the NER process (*26, 27*). NER is the major pathway for the repair of bulky, helix-distorting lesions usually associated with UV light-induced damage.

[1] Address for correspondence: Purdue University, School of Health Sciences, 550 Stadium Mall Drive, West Lafayette, IN 47907-2051; e-mail: trebor@purdue.edu.

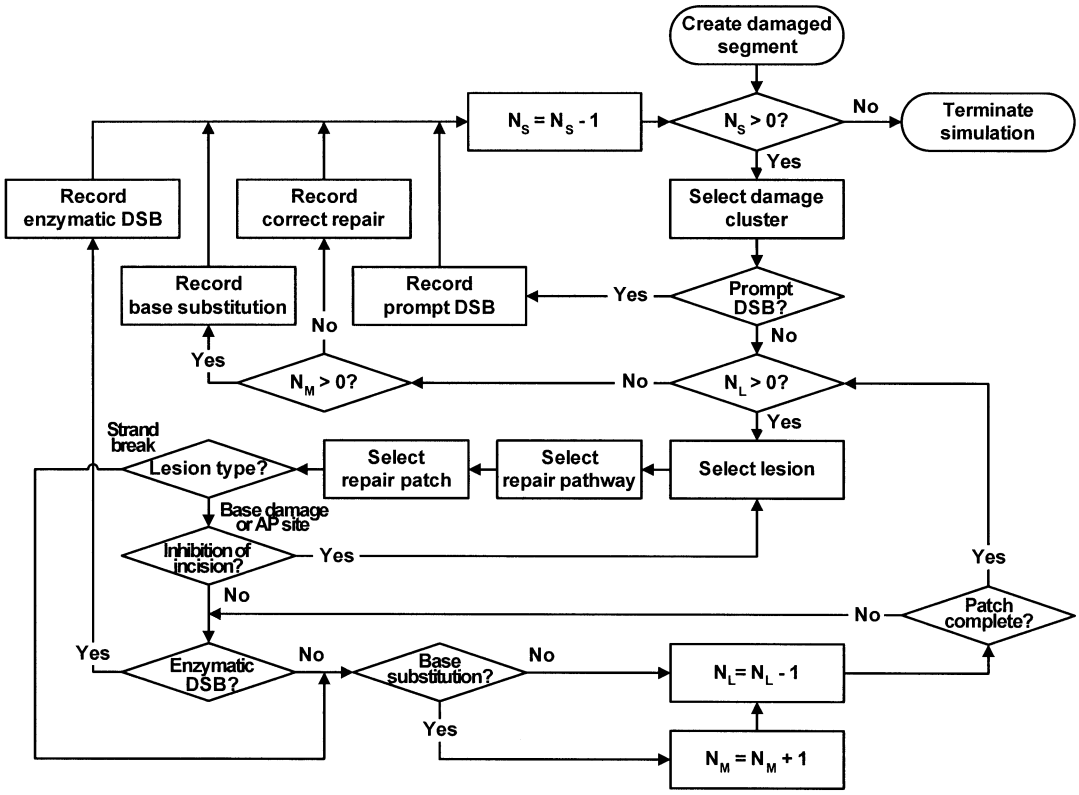


**FIG. 1.** Flowchart of the MCER computer code. $N_S$, number of single or clustered damage sites in the DNA segment; $N_L$, number of lesions in the cluster; $N_M$, number of base substitutions (mutations) accumulated during repair of a cluster.

However, oxidative DNA lesions that are normally considered substrates for BER can also be recognized and repaired by bacterial (*28, 29*), yeast (*30, 31*) and human (*32, 33*) NER pathways. NER is also the primary pathway for the removal of reactive oxygen species-induced cyclopurines in mammalian cells (*34, 35*).

Although the proteins responsible for BER and NER activities differ, both repair processes are accomplished through a similar series of steps that include (1) excision of a damaged base (BER pathway) or damage recognition (NER pathway), (2) incision of the DNA sugar-phosphate backbone and removal of the damaged DNA fragment, (3) gap-filling synthesis by a DNA polymerase, and (4) sealing of the gap by a DNA ligase. Both BER (*25*) and NER (*26*) are highly conserved repair pathways among all eukaryotes, i.e. from yeast to humans. Significant homologies have also been demonstrated among bacterial and human proteins that participate in BER (*36*). The highly conserved nature of the excision repair pathways suggests that many observations in prokaryotes and lower eukaryotes can, in the absence of other information, be reasonably used to make inferences about processes that occur in humans.

Sokhansanj *et al.* (*37*) have developed a mathematical model to predict the kinetics of BER. However, their model does not provide any information about the outcome from excision repair as a function of cluster complexity. We propose for the first time a Monte Carlo excision repair (MCER) model that simulates key steps in the excision repair of all classes of single lesions and clustered lesions other than DSBs, regardless of whether the initial damage is caused by endogenous processes, ionizing radiation or some other physical or chemical agent. The MCER model includes mechanistic details specific to both the short- and long-patch BER pathways as well as the NER pathway. The model allows for pathway interactions by means of probability distributions that specify the relative contribution each pathway makes to the overall repair of DNA damage by excision repair mechanisms. In this article, we describe the MCER model and investigate the properties of the model for the case of DNA damage induced by ionizing radiation. The companion article (*38*) compares model predictions to published data for the conversion of clustered damages into DSBs through enzymatic processes and for the production of point mutations in the human *HPRT* (hypoxanthine guanine phosphoribosyl transferase) gene.

## MCER MODEL

A flowchart summarizing the MCER computer code is shown in Fig. 1. A step-by-step description of key aspects of the model is provided below.

### *Step 1: Create Damaged Segment*

Damage to a cell's entire DNA or any portion of the genome (chromosome, gene, etc.) can be processed by the

MCER model. Input information for the MCER code includes (1) an undamaged nucleotide sequence for one DNA strand (the sequence on the other strand can be determined using base complementarity rules) and (2) the configuration of damaged nucleotides on both strands. All studies reported in this article are based on damage configurations generated using the Monte Carlo damage simulation (MCDS) algorithm (*4*). The MCDS algorithm is capable of generating distributions of base damages and strand breaks for selected types of low-LET (4.5 keV electrons) and high-LET (0.3–4 MeV protons and 2–10 MeV α particles) radiation. Because the MCDS algorithm does not provide any information on the yield of radiation-induced AP sites, this type of damage is not considered in the reported studies. However, the MCER model is designed to process damaged bases, AP sites and strand breaks separately so that all three types of damage can be handled when models to predict the yield and the distribution of radiation-induced AP sites become available.

Human DNA consists of approximately 60% A-T pairs and 40% G-C pairs (*39*), and all of the results reported in this article are based on random nucleotide sequences with this same proportion of A-T and G-C base pairs. However, simulations can also be performed for specific nucleotide sequences [e.g., see the companion article (*38*)].

*Step 2: Select Damage Cluster*

For low-LET radiation, the MCDS algorithm produces approximately 2,300 damage sites $Gy^{-1}$ $cell^{-1}$ [see Table 3 in ref. (*38*)]. For a mammalian cell that contains 6,000 Mbp of DNA, the average distance between adjacent damage sites after 1 Gy of low-LET radiation will be about 2.6 Mbp. This observation suggests that the chance two damage sites will be created close to each other is very small. Even for high-LET radiation, spatially correlated damage clusters formed through intratrack mechanisms are expected to be separated by at least 85 to 200 bp (*40, 41*).

For doses of ionizing radiation less than about 10 to 100 Gy, the average distance between individual or clustered damages is very large compared to the sections of DNA involved in the excision repair process (e.g., patch sizes are typically less than 30 bp; see the discussion in step 6). Considerations such as these suggest that the outcome from the repair of one damage cluster (or single damage) is independent of the outcome from the repair of other clustered damages even if the repair of multiple clusters occurs at the same time. Consequently, the selection of a damage site to repair can be simulated in a computationally convenient order without regard for its location within the DNA. To select a damage cluster to repair, the MCER algorithm scans along the DNA segment until a single damage or a clustered damage site is encountered. The details of the algorithm to select a damage site are described elsewhere (*4*).

*Step 3: Prompt DSBs*

In contrast to DSBs that are formed as a result of DNA repair processes (enzymatic DSBs), DSBs that are formed directly by radiation are referred to as prompt DSBs. If two strand breaks occur on opposite strands of the DNA within distance $N_{dsb}$ (in units of bp), the MCER model records a prompt DSB. Experiments (*42*) suggest that $N_{dsb}$ is of the order of 8 or 9 bp. The value of 10 bp has been used in many modeling studies (*40, 43–45*) that demonstrated good agreement with measured data. Consequently, we have also adopted 10 bp as a default estimate for $N_{dsb}$. Because DSBs cannot be rejoined by the BER or NER pathways, no further analysis of the DSB is performed within the MCER algorithm. Instead, the MCER model proceeds to the next section of damaged DNA segment (step 2). If the damage cluster is not categorized as a prompt DSB, the excision repair process is initiated (step 4).

*Step 4: Select Lesion within the Cluster*

The excision repair process starts by selecting a lesion to target for removal (this step is trivial for isolated damages). The lesion selection process is accomplished in two stages. First, one of the two DNA strands is selected. Then a lesion is selected from that strand. The strand selection process is governed by the probability $P_1$. If $P_1 = 0.5$, both strands have an equal chance to be selected. By increasing or decreasing the value of $P_1$, lesions can be removed preferentially from strand one ($P_1 > 0.5$) or two ($P_1 < 0.5$). In the limit as $P_1$ approaches zero or one, all lesions in the preferred strand will be removed before lesions in the opposing strand are repaired. Such a strand selection procedure can be used to simulate preferential repair of lesions in the transcribed DNA strand, which has been reported for both the NER (*46*) and BER (*47*) pathways. For clusters with more than one damaged nucleotide in the selected strand, the lesion targeted for repair is selected at random. Lesions in the opposing strand are excluded from this selection process.

*Step 5: Select Repair Pathway*

After a damaged nucleotide is targeted for removal, the pathway responsible for removing the lesion is determined. Collectively, steps 4 and 5 represent recognition of the lesion by pathway- and damage-specific repair enzymes. Within the MCER model, short- and long-patch BER are considered distinct pathways because the size of the repair patch has a significant impact on model predictions (see the Results). The relative contribution of each repair pathway to the overall process of removing clustered damages, a form of pathway interaction, is determined by specifying three probabilities: $P_{SP}$, $P_{LP}$ and $P_{NER}$. These branching ratios sum to unity.

The BER mechanism can repair the three types of lesions considered in this work (base damages, AP sites and strand breaks). Although mammalian NER has been reported to

repair many different types of DNA damage, including damaged bases and AP sites (see the Introduction), there is no evidence known to the authors that NER can repair strand breaks that were not themselves generated during NER. Therefore, in the MCER simulations, if the lesion targeted for repair is a base damage or an AP site, the repair pathway is chosen by directly sampling the distribution described by the probabilities $P_{SP}$, $P_{LP}$ and $P_{NER}$. If the lesion targeted for repair is a strand break, the repair pathway is selected from the rescaled distribution:

$$P'_{SP} = \frac{P_{SP}}{P_{SP} + P_{LP}};$$

$$P'_{LP} = \frac{P_{LP}}{P_{SP} + P_{LP}}.$$

In modeling repair pathway interactions, three special cases are of particular interest: (1) all lesions are removed by SP BER ($P_{SP} = 1$, $P_{LP} = 0$, $P_{NER} = 0$), (2) all lesions are removed by LP BER ($P_{SP} = 0$, $P_{LP} = 1$, $P_{NER} = 0$), and (3) all base damages and AP sites are removed by NER ($P_{SP} = 0$, $P_{LP} = 0$, $P_{NER} = 1$) and all strand breaks are removed by LP BER ($P'_{SP} = 0$ and $P'_{LP} = 1$). The combined NER/LP BER repair scenario (no. 3 above) is postulated because of the lack of experimental evidence that NER can repair strand breaks and thus either the SP BER or LP BER pathway must be involved in the repair of any cluster that includes a strand break.

*Step 6: Select Repair Patch*

SP BER is characterized by the replacement of a single (damaged) nucleotide. For LP BER and NER, which involve the removal of more than one nucleotide, simulation of damage excision and DNA resynthesis is repeated for each nucleotide in the repair patch. Nucleotides in the patch are excised and resynthesized sequentially in the direction from the 5′ end to the 3′ end of the DNA strand (the location of the 3′ and 5′ ends for both DNA strands was chosen arbitrarily and is fixed within the MCER code).

In LP BER, the repair patch begins at the location of the damaged nucleotide and is elongated toward the 3′ end of the DNA strand on which the lesion is located. Although repair patches up to 10 nucleotides long have been observed during LP BER reconstituted using human proteins (*48*), the replacement of just two nucleotides is the predominant mode (*49*). Patches 2–4 nucleotides long are detected about 70% of time (*48*). To account for the observed trends, a normalized probability distribution was constructed such that patches 2 and 10 nucleotides in length are the most and least likely to occur, respectively. The probabilities that patches of intermediate size occur were assigned so that they decrease monotonically from 3 to 9 nucleotides, subject to the constraints: (1) The sum of the probabilities for patches 2–4 nucleotides in length equals 0.7 and (2) the sum of the probabilities for patches 5–10 nucleotides in length equals 0.3. The resulting distribution is shown in Fig. 2A. The MCER algorithm samples this distribution to obtain the size of the fragment replaced by the LP BER pathway.

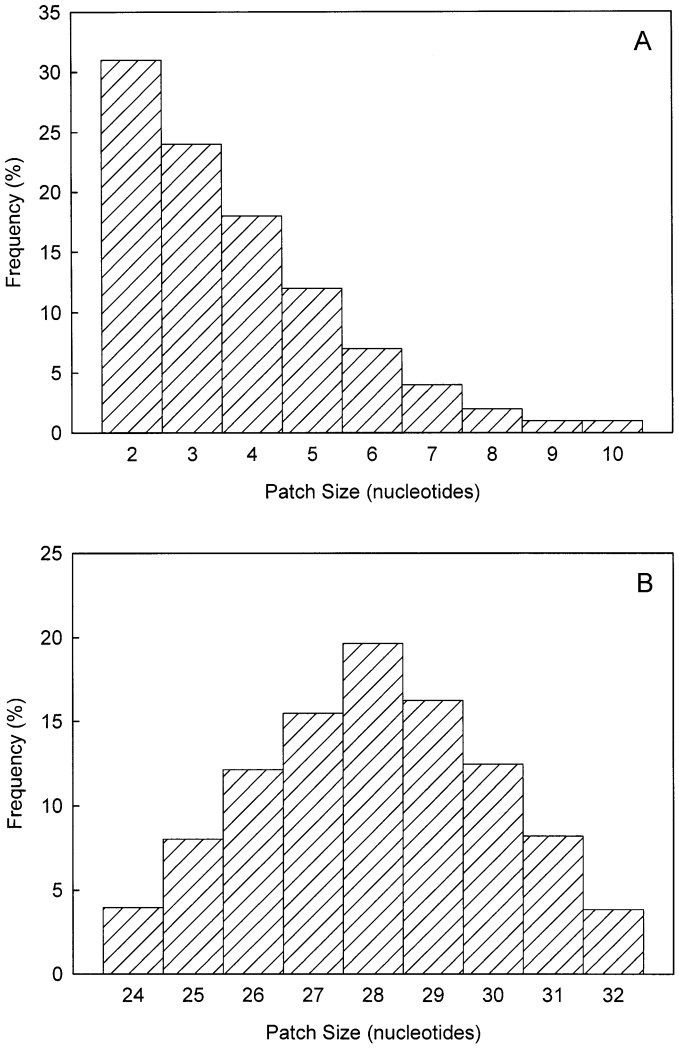


**FIG. 2.** Patch-size distributions used in the MCER model. Panel A: LP BER (average patch size is 3.7 nucleotides). Panel B: NER (average patch size is 28 nucleotides).

During eukaryotic NER, incision of the DNA backbone usually occurs between the 2nd through the 10th phosphodiester bond 3′ to the damage site and between the 16th through the 26th phosphodiester bond 5′ to the damage site (*26, 27*). In the NER simulations, two incision points on either side of the damaged nucleotide are selected, and the oligonucleotide fragment between the two incision points is removed and resynthesized. The incision points are determined by randomly sampling positions 3–7 nucleotides on the 3′ side of the lesion and 20–24 nucleotides on the 5′ side of the lesion. The resulting patch-size distribution is shown in Fig. 2B. This distribution is consistent with the reports that 24–32-nucleotide fragments are excised in eukaryotes with the most frequent patches 27–29 nucleotides long (*26*).

*Step 7: Lesion Type*

To simplify the model, we assume that the repair process cannot be interrupted or compromised prior to the incision of the DNA backbone. Simulation of the following steps in the excision repair mechanism is performed explicitly and depends on the type of lesion processed. If the lesion targeted for removal is a strand break, the DNA incision step is not required. Therefore, inhibition of DNA incision (step 8) cannot occur and an enzymatic DSB cannot be formed by incision of that strand (step 9). If a strand break has been targeted for removal, the next step in the repair process is the simulation of DNA resynthesis (step 10). If the lesion targeted for removal is a damaged base or an AP site, all three simulation steps (steps 8–10) are performed.

*Step 8: Inhibition of DNA Incision*

Several research groups studied BER of two closely spaced lesions on the same or opposing DNA strands [see refs. (*50*) and (*51*) for reviews]. These studies show that the excision of a damaged base followed by the incision of the DNA strand may be inhibited by the presence of additional damage on the opposite strand. A pronounced inhibitory effect is observed if the opposed lesion is a strand break or an AP site, but not a damaged base (*52–55*). Because AP endonucleases rapidly convert AP sites to strand breaks in XRS5 nuclear extracts, David-Cordonnier *et al.* (*54*) concluded that the lesion causing the observed inhibitory effect is a strand break. This phenomenon is simulated in the MCER model by specifying an inhibition distance, $N_{inh}$ (bp). That is, repair of a base damage or an AP site is inhibited when a strand break is detected on the opposite strand within $N_{inh}$. If inhibition occurs, the simulation returns to step 4 and selects another lesion to remove from the cluster.

Blaisdell *et al.* (*56*) report that the BER processing of a damaged base (8-oxoG) is inhibited if a strand break is present on the opposite DNA strand within 3 bp. If the strand break is 3 bp or more away, a DSB may be formed. Based on this information, a default value of $N_{inh} = 3$ bp is used in the MCER model. No reports of the inhibitory effect are known to the authors for NER, and thus $N_{inh} = 0$ is always used for the NER pathway.

*Step 9: Enzymatic DSBs*

For some damage configurations, an unrepaired strand break may be present opposite a damaged base or an AP site that has been targeted for removal. If, during the removal of these two types of lesions, the DNA backbone is incised to form a gap close to an existing strand break in the opposing strand, an enzymatic DSB will be formed. An enzymatic DSB will be formed only when the newly created strand break is located farther away than $N_{inh}$ base pairs from the break in the opposing strand. The same parameter $N_{dsb}$ that was used to classify clustered damages as prompt DSBs is used to designate the maximum separation between the enzymatic cut and the strand break such that a DSB is formed. If a DSB is formed through this mechanism, the event is recorded as an ''enzymatic DSB'' and repair of the cluster is aborted because the BER and NER pathways do not process DSBs. Otherwise, the repair simulation proceeds to the DNA synthesis step (step 10).

Because the MCER algorithm includes a prompt DSB detection procedure (step 2), strand breaks targeted for removal by excision repair cannot result in the formation of an enzymatic DSB. That is, if a strand break is present in the opposite strand within distance $N_{dsb}$, the MCER model classifies the cluster as a prompt DSB and excision repair is not possible. Thus, for the repair of strand breaks, two mutually exclusive outcomes are possible: correct repair (no base substitutions) and repair with at least one base substitution (mutation). The excision repair of base damages and AP sites may result in one of three mutually exclusive events: correct repair, repair with a mutation, or formation of an enzymatic DSB.

*Step 10: Base Substitution*

The MCER model assumes that base substitutions may be created during the gap-filling synthesis step of the excision repair process. The model does not explicitly account for the formation of insertion- or deletion-type mutations. Details such as these can be easily incorporated into the Monte Carlo repair scheme in the future, although additional parameters would need to be introduced into the modeling process.

The MCER model allows for the possibility that DNA polymerases insert a non-complementary nucleotide opposite an undamaged template due to their intrinsic tendency to err. The polymerase error rates are usually very small and may vary by several orders of magnitude ($10^{-4}$–$10^{-7}$ per incorporated deoxynucleotide) depending on the properties of the polymerase (*57*). The identity of DNA polymerases that perform gap-filling synthesis in mammalian excision repair is well known. Polymerase β is the major player in the SP BER pathway (*58, 59*). Polymerases δ and/or ε synthesize repair patches in both LP BER (*59, 60*) and NER (*61*). Error rates of the order of $10^{-4}$ have been reported for one-nucleotide gap filling by polymerase β (*62, 63*) with one suggestion of a lower error rate ($\sim 10^{-5}$) (*64*). Polymerase β lacks the $3' \rightarrow 5'$ exonuclease activity that can correct mistakes and enhance polymerase fidelity (*57*). The fidelity of polymerases δ and ε during replicative synthesis is considerably higher (*65*) because these polymerases possess $3' \rightarrow 5'$ exonuclease activity. Exonucleolytic proofreading contributes about two orders of magnitude to fidelity (*57*). We have adopted the following characteristic polymerase error rates: $10^{-4}$ for polymerase β and $10^{-6}$ for polymerases δ/ε. Within the MCER model, the pathway-specific probabilities that a base substitution occurs opposite an undamaged nucleotide are thus $\eta_{SP} = 10^{-4}$ and $\eta_{LP} = \eta_{NER} = 10^{-6}$ per synthesized nucleotide.

**TABLE 1**
**Input Parameters for the MCER Model**

| Parameter | Description | Default value |
|---|---|---|
| $N_{dsb}$ | Maximum distance between two strand breaks to form a DSB | 10 bp |
| $N_{inh}$ | Distance over which the inhibitory effect takes place | 3 bp |
| $P_1$ | Probability of choosing a lesion from the first DNA strand | 0.5 |
| $\eta_{SP}$ | Polymerase error rate for SP BER (polymerase β) | $10^{-4}$ |
| $\eta_{LP}$ | Polymerase error rate for LP BER (polymerases δ/ε) | $10^{-6}$ |
| $\eta_{NER}$ | Polymerase error rate for NER (polymerases δ/ε) | $10^{-6}$ |
| $\varphi_{Bd}$ | Probability of incorrect nucleotide insertion opposite a base damage | 0.75 |
| $\varphi_{Bl}$ | Probability of incorrect nucleotide insertion opposite an AP site | 0.75 |

*Note*. The value of the parameter $\varphi_{Bl}$ does not affect the results reported in this work because AP sites are absent from the input data stream provided by the MCDS algorithm.

When the template for DNA synthesis contains a damaged base or an AP site, the chance an incorrect base will be inserted will most likely be higher than the baseline error rates ($10^{-4}$–$10^{-6}$) expected when the template is undamaged. In the MCER model, DNA polymerases cannot encounter a strand break, because this type of clustered damage must be a DSB and excision repair of such a cluster is aborted. To simulate DNA synthesis when the template is damaged, the MCER model by default assumes a scenario in which a damaged base or an AP site directly opposite the repaired nucleotide is completely non-instructional for all DNA polymerases that perform DNA synthesis during excision repair. Therefore, one of the four nucleotides (A, T, G or C) is inserted opposite AP sites and damaged bases at random. This random insertion process is simulated by setting parameters $\varphi_{Bd}$ and $\varphi_{Bl}$ that describe the probability of nucleotide misinsertion to 0.75. The subscripts *Bd* and *Bl* denote base damages and sites of base loss (AP sites), respectively.

For both modes of creating a base substitution, the identity of the misinserted nucleotide is determined by random sampling from the pool of three incorrect nucleotides. The total number, location and type of base substitutions are determined by comparing the base sequence before and after repair. If at least one base substitution is created during the repair process, the cluster is classified as ''repaired with mutation.'' Otherwise, the cluster is classified as ''correctly repaired.''

*Step 11: Patch Complete*

The excision and DNA synthesis steps are performed for each nucleotide in the repair patch. The MCER algorithm tests for the creation of an enzymatic DSB or a base substitution after the removal of each nucleotide. When the replacement of all nucleotides within the repair patch is completed, the repair simulation returns to step 4 and selects the next damaged nucleotide to target for repair. We assume that the DNA ligation step in BER and NER is error-free and can thus be neglected.

Within the MCER model, the lesions that form a cluster are processed sequentially; i.e., the replacement of all nucleotides within the repair patch must be completed before the repair of any other lesion within the cluster is initiated. Others (*50, 66*) have also hypothesized that the repair of clustered damage sites involves the sequential processing of individual damages. The sequential repair of lesions within a cluster leads to the concept of repair cycles. A repair cycle begins with the selection of a lesion to repair (step 4) and ends with either the formation of an enzymatic DSB (step 9) or the replacement of all nucleotides within the repair patch (step 11). We hypothesize that, if damage recognition is the key rate-limiting step in BER and NER and if all repair proteins disassociate from the DNA after completing the repair patch, the relative time to complete the repair of a clustered damage site will increase in direct proportion to the number of repair cycles. This hypothesis implies that the time required to completely remove a cluster will tend to increase as cluster complexity (number of damaged nucleotides per cluster) increases.

*Step 12: Terminate Simulation*

Program execution terminates when all damage in the DNA segment has been processed. Clustered damages that were not classified as prompt DSBs are sorted into three categories according to the excision repair outcome: (1) correctly repaired clusters, (2) clusters repaired with mutations, and (3) clusters converted into DSBs. The yield of each class of damage is tabulated as a function of the number of lesions per cluster. The number of repair cycles required to remove each class of damage is also tabulated.

## RESULTS

To gain insight into the properties of the model, the results of a series of parameter sensitivity studies are presented. Except where explicitly stated otherwise, the default parameter values summarized in Table 1 are used in the simulations. Results that list low-LET radiation and high-LET radiation as a source of DNA damage have been obtained using the MCDS algorithm for 4.5 keV electrons and 2 MeV α particles, respectively. The characteristics of clustered damages formed by these two types of radiation (e.g., cluster length and the number of damaged nucleotides per

cluster) have been estimated using the MCDS algorithm and published elsewhere (*4*).

### *Effects of LET and Cluster Complexity*

Figure 3 shows the probability of three mutually exclusive repair outcomes, i.e. correct repair, repair with a mutation, and repair resulting in a DSB, as a function of the number of lesions per cluster. As expected, the results shown in Fig. 3A indicate that the probability of error-free repair decreases rapidly as cluster complexity increases. The probability an enzymatic DSB is formed (Fig. 3C) increases as cluster complexity increases. For the SP BER pathway, the probability a mutation is formed (Fig. 3B) increases slightly for clusters composed of 2 to 8 damaged nucleotides and then remains approximately constant up to 15 lesions per cluster. For the NER/LP BER simulations, the probability a mutation is formed increases until the number of lesions per cluster reaches 5 or 6 and then begins to decrease. For clusters composed of many lesions, enzymatic DSB formation competes with the creation of mutations. Because DNA incision occurs earlier in the excision repair process than DNA synthesis, the formation of an enzymatic DSB occurs before and thus takes precedence over mutations. Consequently, the DSB formation probability continues to increase with increasing cluster complexity while the probability of creating a mutation reaches a maximum and then begins to decrease.

The model predicts that clusters containing the same number of lesions have similar repair characteristics, regardless of whether the initial damage was induced by low-LET radiation or high-LET radiation. However, the spectra of clustered damages formed by 4.5 keV electrons and 2 MeV $\alpha$ particles are quite different [refer to Fig. 7 in ref. (*4*)]. Compared to electrons, $\alpha$ particles tend to create clusters of greater complexity. Spectrum-averaged repair probabilities can be obtained by multiplying the probability that a specific repair outcome occurs for each type of cluster by the yield of that cluster and then summing over all classes of damage. The spectrum-averaged probabilities of the three repair outcomes for low- and high-LET radiation are shown in Table 2. These data clearly indicate the differences between low-LET and high-LET radiation. The model predicts that the overall probability of correct repair decreases substantially as particle LET increases, as expected. Regardless of the repair scenario, the spectrum-averaged probabilities of the two deleterious outcomes (i.e. mutations and enzymatic DSBs) increase as particle LET increases.

For all three repair outcomes, the predicted outcome from the SP BER pathway is always more favorable to a cell than the outcomes from the combined NER/LP BER scenario. That is, for all classes of damage, the MCER model predicts that the probability of correct repair is higher and the probability of mutation induction or DSB formation is lower for SP BER than for the NER/LP BER scenario. Repair probabilities for the LP BER pathway are intermediate between the results for the SP BER and NER/LP BER scenarios.

### *Effects of Preferential Repair of Lesions in One DNA Strand ($P_1$ parameter)*

The effects of preferential repair of lesions in one strand of the DNA as a function of cluster complexity are shown in Fig. 4 for the bounding cases represented by the SP BER and NER/LP BER scenarios. Because the predicted repair outcomes are similar for low- and high-LET radiation as long as the number of damaged nucleotides forming the cluster is the same (refer to Fig. 3), results are shown only for low-LET radiation. The curves for the default parameter value of $P_1 = 0.5$ are the same as the correspondingly marked curves in Fig. 3. The data for $P_1 = 0$ show the maximum possible effect of preferential repair predicted by the MCER model for the SP BER and NER/LP BER scenarios. Note that, because of symmetry in DNA damage configurations, parameter values $P_1$ and $(1 - P_1)$ can be expected to yield the same results within statistical variations. Interestingly, the transition from choosing lesions at random from both strands ($P_1 = 0.5$) to selectively removing lesions from one strand ($P_1 = 0$ or $P_1 = 1$) reduces the chance an enzymatic DSB will be formed (Fig. 4C) and increases the chance a mutation will be created (Fig. 4B). However, the preferential removal of damage from one strand increases the probability of correct restitution (Fig. 4A), which indicates that the overall effects of preferential damage removal may be beneficial to a cell. The preferential repair of damage in the transcribed DNA strand may occur during transcription-coupled repair (*67*).

### *Effects of Inhibition of DNA Incision ($N_{inh}$ parameter)*

Figure 5 shows the effects of the inhibition distance parameter, $N_{inh}$, on model predictions for low-LET radiation. Repair outcome probability curves are presented for $N_{inh} = 3$ (default parameter), $N_{inh} = 0$ (absence of the inhibitory effect), and $N_{inh} = 6$ to show the effects of a possible twofold increase in the inhibition distance. For SP BER, the inhibitory effect reduces the chance an enzymatic DSB will be formed (Fig. 5C) but leads to an increase in the number of clusters repaired with mutations (Fig. 5B). The latter prediction supports the hypothesis that inhibition of excision repair of clustered damage sites could result in increased mutation frequencies (*16*). The probability of correct repair increases as the magnitude of the inhibitory effect increases, i.e., as the values selected for the $N_{inh}$ parameter become larger (Fig. 5A). The NER/LP BER scenario is not sensitive to the value of $N_{inh}$ because base damages that require the DNA incision step are repaired through NER in that scenario, and the MCER model assumes that DNA incision in the NER pathway cannot be inhibited. Therefore, only one set of NER/LP BER curves is presented for comparison with the SP BER data. When $N_{inh} = 0$, the probability of DSB formation by SP BER approaches

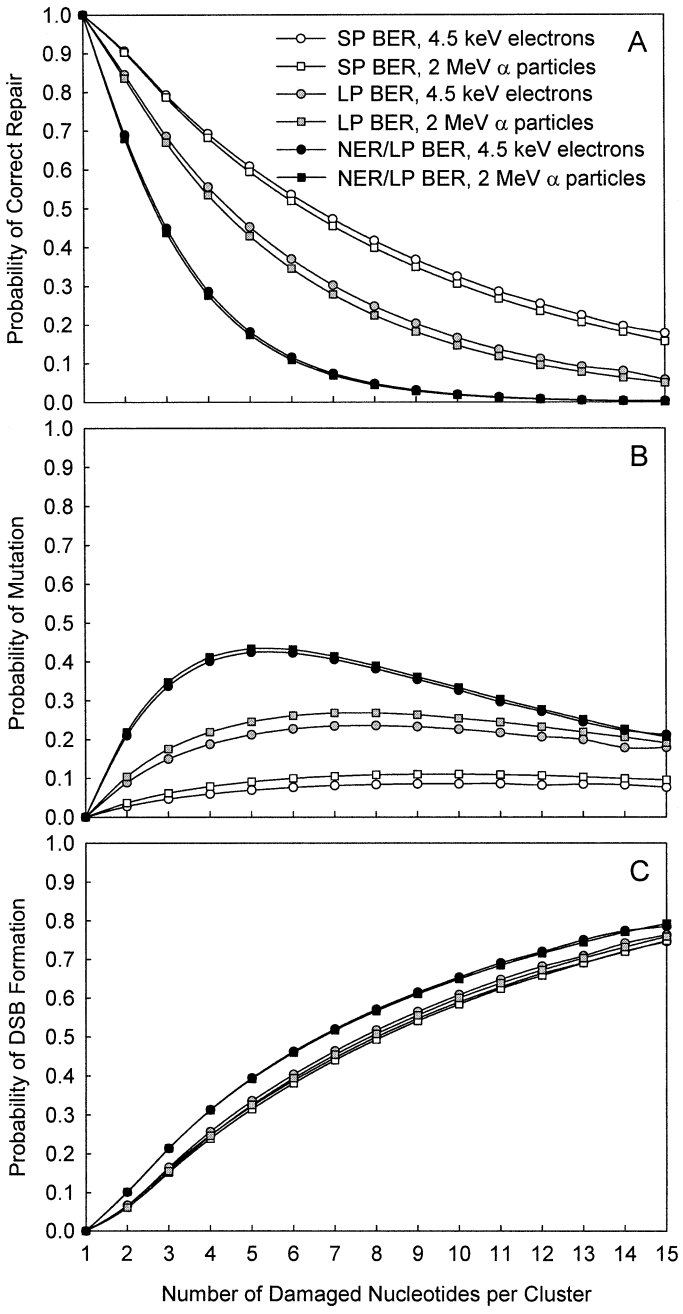


**FIG. 3.** Effects of cluster complexity (number of damaged nucleotides per cluster) and particle LET. The yields of clusters in each repair category (correct repair, repair with a DSB, and repair with a mutation) were obtained by averaging results of $10^7$ simulations for a 1-Gy dose of low-LET radiation (4.5 keV electrons) and $10^5$ simulations for a 1-Gy dose of high-LET radiation (2 MeV α particles). Probabilities of repair outcomes were calculated by dividing the average yields of clusters in each repair category by the total number of clusters that were not classified as prompt DSBs. Symbols represent MCER simulation results and are connected with smooth lines to guide the eye.

the probability of DSB formation for the combined NER/LP BER scenario. This implies that the DSB formation process, which is directly affected by the $N_{inh}$ parameter, is independent of the repair pathway in the absence of the inhibitory effect.

*Effects of DNA Synthesis Opposite a Damaged Template ($\varphi_{Bd}$ parameter)*

The sensitivity of model predictions to alternative assumptions about the mechanisms of DNA synthesis opposite a damaged base is shown in Fig. 6 for low-LET radiation. Two sets of curves for the extreme values of the $\varphi_{Bd}$ parameter are shown, one for $\varphi_{Bd} = 1$, which is equivalent to an assumption that DNA polymerases always insert a non-complementary nucleotide opposite a damaged template, and another for $\varphi_{Bd} = 0$; i.e., DNA polymerases always insert the correct nucleotide when the lesion in the opposing strand is a base damage. Results for the default parameter value of 0.75 are also shown for comparison.

The value of the $\varphi_{Bd}$ parameter directly affects model predictions related to the production of mutations (Fig. 6B). Simulation results for $\varphi_{Bd} = 1$ provide an upper bound on the probability a mutation is created. In both repair scenarios, model predictions for $\varphi_{Bd} = 0$ in Fig. 6B are indistinguishable from the abscissa, which indicates that the lower bound for the probability of creating a mutation is close to zero (the probability is not exactly zero because polymerases may still create a base substitution even when the template for DNA synthesis is undamaged). The probability of DSB formation (Fig. 6C) is not affected by the $\varphi_{Bd}$ parameter because the DNA synthesis step cannot produce any additional DSBs, nor can it limit their formation. In Fig. 6A, the probability of correct repair decreases as cluster complexity increases even if we assume that DNA polymerases always insert the correct nucleotide opposite damaged bases ($\varphi_{Bd} = 0$). For the latter case, the probability of creating a mutation approaches zero, and thus the probability of correct repair is governed solely by the probability of DSB formation, which increases with increasing cluster complexity regardless of the value selected for the $\varphi_{Bd}$ parameter.

*Effects of DNA Synthesis Opposite an Undamaged Template ($\eta_{SP}$, $\eta_{LP}$ and $\eta_{NER}$ parameters)*

The results shown in Figs. 3–6 account for base substitutions that occur because DNA polymerases sometimes insert an incorrect nucleotide even when the template for DNA synthesis is undamaged. This process is described by the polymerase error rates $\eta_{SP} = 10^{-4}$ and $\eta_{LP} = \eta_{NER} = 10^{-6}$. However, when these parameters are set to zero ($\eta_{SP} = \eta_{LP} = \eta_{NER} = 0$), the predicted outcomes are nearly identical to the ones shown in Figs. 3–6 (data not shown). This result implies that a DNA polymerase's intrinsic tendency to err has a negligible impact on the predicted mutation yield. For ionizing radiation-induced DNA damage, the model predicts that the principal mechanism for the formation of mutations is DNA synthesis opposite damaged template.

*Repair Cycles*

Because LP BER and NER involve the removal of patches several nucleotides in length, these pathways may some-

**TABLE 2**
**Repair Outcome Probabilities Averaged over all Types of DNA Damage**

| | Probability of correct repair | | Probability of mutation | | Probability of DSB formation | |
|---|---|---|---|---|---|---|
| Repair scenario | 4.5 keV electrons | 2 MeV α particles | 4.5 keV electrons | 2 MeV α particles | 4.5 keV electrons | 2 MeV α particles |
| SP BER | 0.951 | 0.791 | 0.012 | 0.048 | 0.037 | 0.161 |
| LP BER | 0.923 | 0.706 | 0.039 | 0.129 | 0.038 | 0.165 |
| NER/LP BER | 0.861 | 0.565 | 0.087 | 0.232 | 0.052 | 0.203 |

times remove more than one damaged nucleotide during a repair cycle. Consequently, a pathway that has larger repair patches may be able to remove a cluster of lesions faster than a pathway that removes smaller fragments. That is, fewer repair cycles may be required to remove a cluster by LP BER, and especially by NER, than by SP BER. The time required to repair a cluster is expected to increase as the number of repair cycles increases. The MCER model thus provides data to estimate pathway-specific relative repair rates for different classes of damage.

Figure 7 shows the average number of repair cycles as a function of the number of damaged nucleotides per cluster. The results shown are for damage configurations representative of low-LET radiation. In all three repair scenarios, the number of cycles to repair a cluster comprised of many lesions approaches a constant. This trend is observed because the processing of very complex clusters by excision repair almost inevitably results in the formation of an enzymatic DSB (Fig. 3C). Thus this asymptotic value can be interpreted as the average number of repair cycles before an enzymatic DSB is created and the excision repair process is aborted. The corresponding curves for 2 MeV α particles (not shown) are similar to the data for low-LET radiation. However, the spectrum-average number of repair cycles is different for low- and high-LET radiation: 1.5 and 2.7, respectively, for the SP BER scenario and 1.2 and 1.7 for the NER/LP BER scenario. These results suggest that the overall half-time for damage repair tends to increase (the repair rate tends to decrease) as the particle LET increases.

## DISCUSSION

At present, the data available in the literature are not sufficient to obtain accurate estimates for the relative contribution each repair branch makes to the overall excision repair process, i.e., identify precise values or distributions of $P_{SP}$, $P_{LP}$ and $P_{NER}$ parameters. Dianov *et al.* (*68*) report that, in human cells, the majority of isolated thymine glycols are removed by SP BER, and the NER and LP BER pathways play a relatively minor role. Fortini *et al.* (*69*) observed similar trends in the repair of another common oxidative lesion, 8-oxoG. These observations are consistent with earlier findings that demonstrate that BER is usually accomplished via the single-nucleotide repair mechanism in both prokaryotes and eukaryotes (*70–72*). SP BER appears to be the major mechanism for the repair of isolated damages while LP BER and NER may serve as backup systems to SP BER. However, LP BER and NER may play a more significant role in the repair of clustered damage. Closely spaced AP sites on opposing strands can create significant distortions in the structure of the DNA (*73*). If accompanied by covalent modifications (*74*), distortions such as these may be large enough to initiate NER of the clustered damage site. Clustered damage may also serve as a signal to switch from SP BER to LP BER. Additional experimental work is needed to identify the pathways and events that determine if and how different types of clustered damage sites are removed by BER and NER.

Because of the uncertainties associated with the interplay between BER sub-pathways and NER, the results reported in this article are presented in terms of hypothetical scenarios that define the range of possible repair outcomes. The three repair scenarios considered are (1) all damage processed by SP BER, (2) all damage processed by LP BER, and (3) damage processed by NER (all damaged bases and AP sites) and LP BER (all strand breaks). The combined NER/LP BER repair scenario is postulated because of the lack of experimental evidence that NER can repair strand breaks.

The model predicts that repair scenarios with longer patches increase the probability of creating a mutation (Fig. 3B) and result in more enzymatic DSBs being produced (Fig. 3C) compared to SP BER. Indeed, Vispé and Satoh (*75*) have demonstrated experimentally that repair through the LP BER pathway leads to an increase in the DSB yield compared to repair through SP BER. This result was attributed to the fact that longer repair patches produced by LP BER may overlap during the repair process and thus increase the chance a DSB will be formed. Following this logic, the NER pathway, which produces even larger repair patches, may be even more harmful to a cell because of the formation of potentially lethal DSBs.

Repair through SP BER may act as a mechanism to protect cells from the DSBs that might otherwise be formed by pathways that produce longer repair patches (*76*). Another DSB protection mechanism may involve sequential processing of clustered damage (*66*). Preferential repair of lesions on one DNA strand and the inhibitory effect, both of which have been demonstrated to limit the formation of

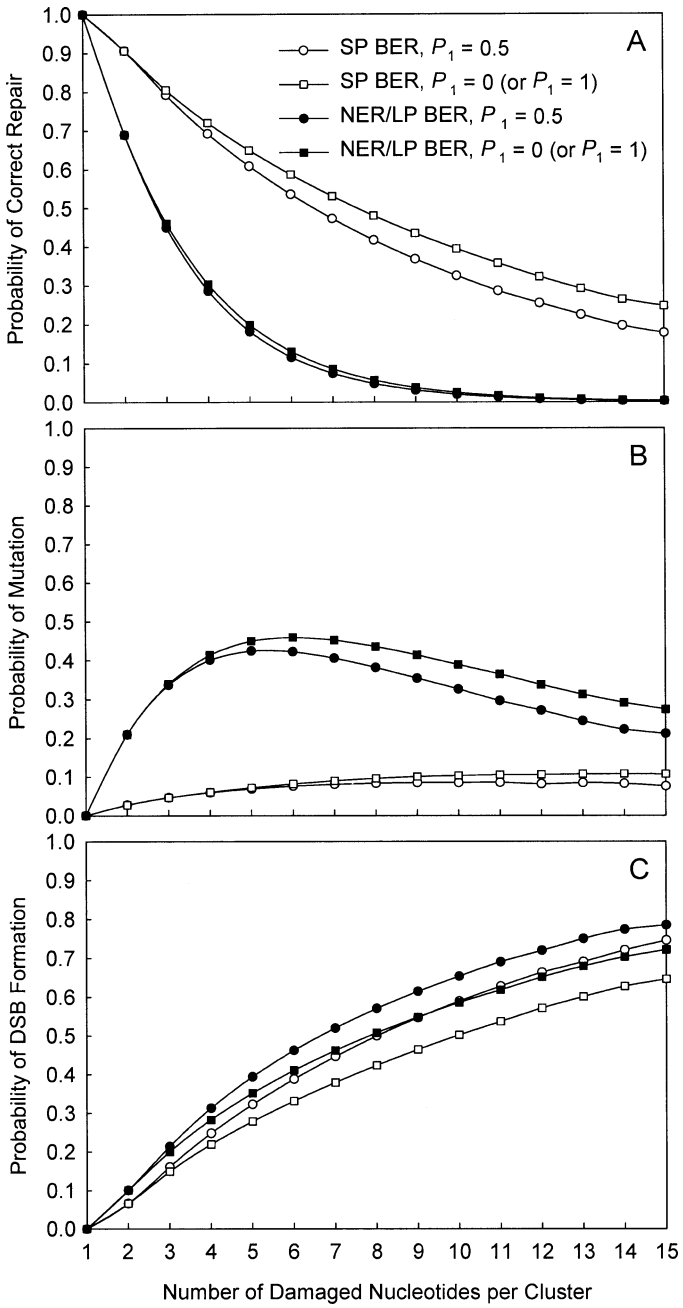


**FIG. 4.** Effects of preferential repair of lesions in one DNA strand. For each combination of model parameters, $10^7$ simulations equivalent to a 1-Gy dose of 4.5 keV electrons were performed. Probabilities of repair outcomes were calculated by dividing the average yields of clusters in each repair category by the total number of clusters that were not classified as prompt DSBs. Symbols represent MCER simulation results and are connected with smooth lines to guide the eye.

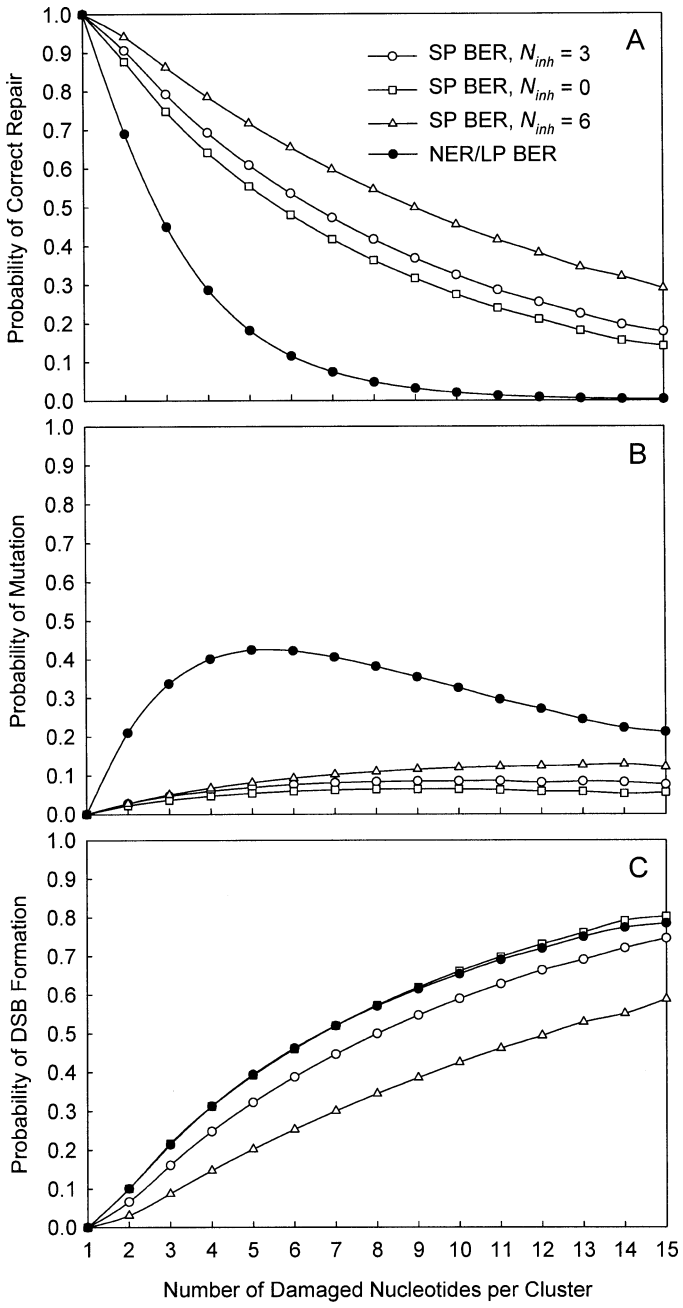


**FIG. 5.** Effects of inhibition of DNA incision. For each combination of model parameters, $10^7$ simulations equivalent to a 1-Gy dose of 4.5 keV electrons were performed. Probabilities of repair outcomes were calculated by dividing the average yields of clusters in each repair category by the total number of clusters that were not classified as prompt DSBs. Symbols represent MCER simulation results and are connected with smooth lines to guide the eye.

DSBs in our simulations (Figs. 4C and 5C, respectively), possibly represent specific manifestations of a more general phenomenon aimed at maintaining genome stability.

DNA synthesis past a wide variety of damages has been studied *in vitro* and *in vivo* [see ref. (*77*) for a review]. The details of the damage bypass process depend on the nature of the lesion (e.g., AP site or thymine glycol), the DNA polymerase used, and the base sequence where the damage site is located (*77*). Although many major oxidative damages, including 8-oxoG, are readily bypassed, AP sites and thymine glycols are a strong block to at least some DNA polymerases [see Table I in ref. (*36*)] and are potentially lethal. However, even strongly blocking lesions can be bypassed and result in a mutation (*36*). In the MCER model, we have assumed that AP sites as well as all types of base

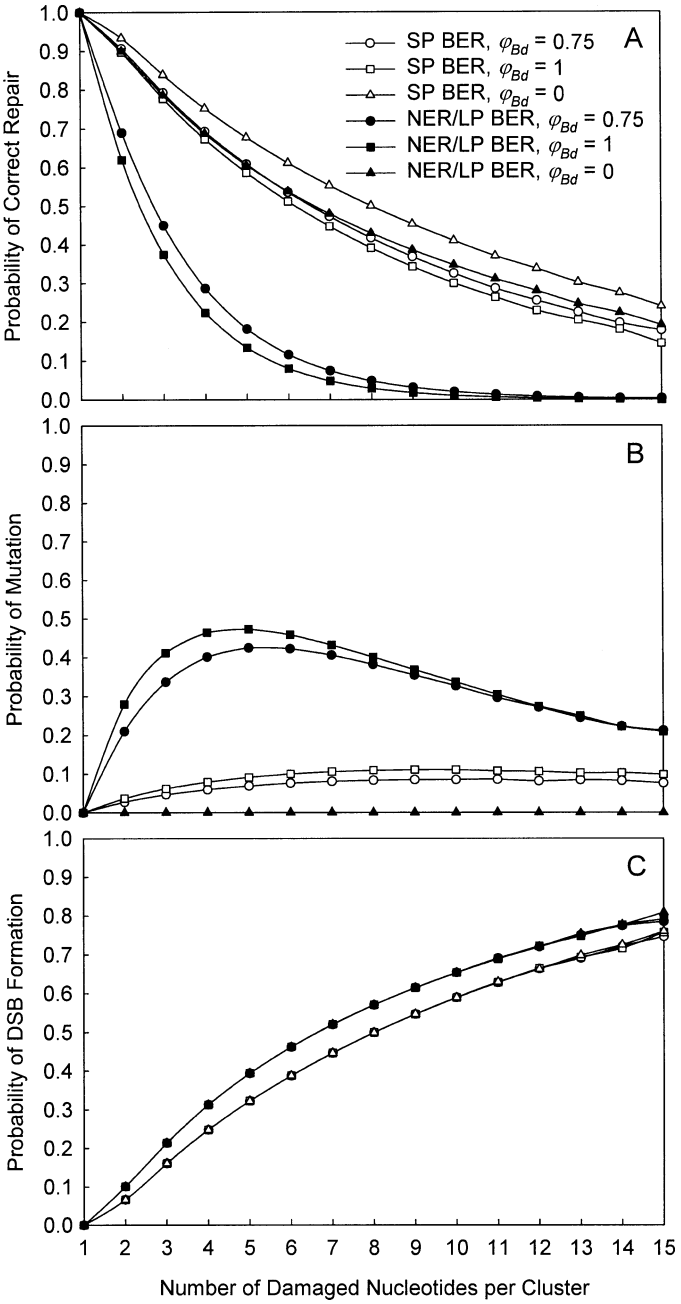


**FIG. 6.** Effects of DNA synthesis past a damaged nucleotide. For each combination of model parameters, $10^7$ simulations equivalent to a 1-Gy dose of 4.5 keV electrons were performed. Probabilities of repair outcomes were calculated by dividing the average yields of clusters in each repair category by the total number of clusters that were not classified as prompt DSBs. Symbols represent MCER simulation results and are connected with smooth lines to guide the eye.

damage can be bypassed efficiently during repetitive cycles of excision repair and are potentially mutagenic.

In contrast to the repetitive cycles of repair postulated in this work, Pearson *et al.* (*17*) have shown for *Escherichia coli* that translesion synthesis followed by mismatch repair plays a significant role in the removal of 8-oxoG with uracil in the opposing strand. The hypothesis is that inhibition of repair within a clustered damage site allows the lesions to

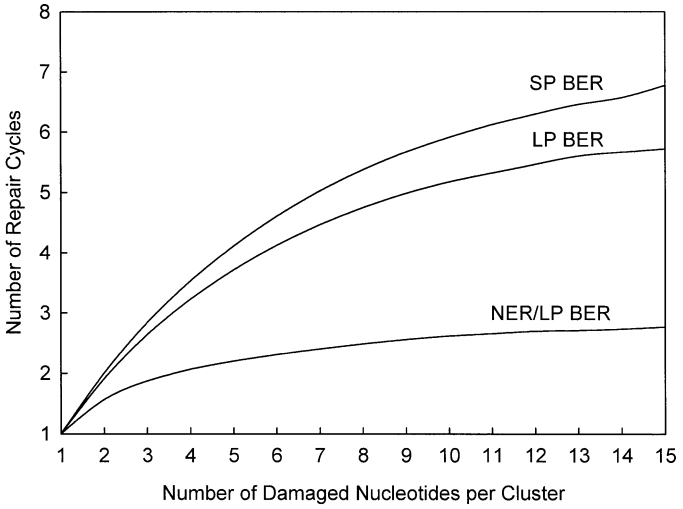


**FIG. 7.** Number of repair cycles as a function of the number of damaged nucleotides per cluster. Results were averaged over $10^7$ simulations for a 1-Gy dose of 4.5 keV electrons.

persist until DNA replication occurs (*17*). Although post-replicative repair is an important mechanism for the processing of clustered damage in bacterial cells, whether this mechanism is also important in mammalian cells is unclear. *E. coli* typically divides in 20–100 min compared to 10 h or more for mammalian cells. This observation implies that a large fraction of clustered damage induced by radiation may need to persist in the DNA for an extended period before post-replication repair could occur. This expectation appears counter to the damage repair kinetics observed in mammalian cells (*78*). Also, mammalian cells with unrepaired DNA damage may initiate apoptosis to avoid, presumably, the consequences of highly mutagenic repair. Several studies show that apoptosis is triggered by the replication of damaged DNA [for a review, see ref. (*79*)]. Additional experimental information is needed to determine whether the clustered damages formed by ionizing radiation are processed by repetitive rounds of excision repair, by post-replication repair, or by a combination of mechanisms.

The MCER model predicts that nearly all single damages are repaired correctly regardless of the values chosen for model parameters (Figs. 3–6). This result is consistent with the notion that the cell killing and mutagenic effects of isolated strand breaks and base damages are inconsequential compared to those of clustered damage sites (*3*, *14*, *15*). Studies with clusters composed of two damaged bases on the opposite DNA strands (*16*, *17*) provide experimental support for the hypothesis that clustered damages are more mutagenic than isolated lesions.

The number of repair cycles is hypothesized to be proportional to the average lifetime of the cluster. Results shown in Fig. 7 indicate that it takes more time to remove clustered damages from the DNA than to remove single damages. In agreement with this observation, experiments show that rates of repair of thymine glycol opposite an AP site (*80*) and 8-oxoG opposite a strand break (*81*) are re-

duced severalfold compared to the rates of repair of single base damages.

We have proposed for the first time a general Monte Carlo framework to simulate the excision repair of DNA damage other than DSBs.[2] Useful insights into the trends predicted by the model are presented in a series of sensitivity studies. Because none of the mechanisms postulated in the MCER model are specific to ionizing radiation, the model may also be useful for predicting repair outcomes for endogenous processes and other DNA-damaging agents.

## ACKNOWLEDGMENTS

This work is supported by the Office of Science (BER), U.S. Department of Energy, Grant Nos. DE-FG02-03ER63541, DE-FG02-03ER63665, KP1102020 42668, and KP1102020 42699.

Received: December 6, 2004; accepted: March 3, 2005

## REFERENCES

1. J. F. Ward, DNA damage produced by ionizing radiation in mammalian cells: Identities, mechanisms of formation, and reparability. *Prog. Nucleic Acid Res. Mol. Biol.* **35**, 95–125 (1988).
2. E. C. Friedberg, G. C. Walker and W. Siede, *DNA Repair and Mutagenesis*, pp. 1–58. ASM Press, Washington, DC, 1995.
3. D. T. Goodhead, Initial events in the cellular effects of ionizing radiations: Clustered damage in DNA. *Int. J. Radiat. Biol.* **65**, 7–17 (1994).
4. V. A. Semenenko and R. D. Stewart, A fast Monte Carlo algorithm to simulate the spectrum of DNA damages formed by ionizing radiation. *Radiat. Res.* **161**, 451–457 (2004).
5. P. V. Bennett, N. S. Cintron, L. Gros, J. Laval and B. M. Sutherland, Are endogenous clustered DNA damages induced in human cells? *Free Radic. Biol. Med.* **37**, 488–499 (2004).
6. K. M. Prise, C. H. L. Pullar and B. D. Michael, A study of endonuclease III-sensitive sites in irradiated DNA: Detection of α-particle-induced oxidative damage. *Carcinogenesis* **20**, 905–909 (1999).
7. J. R. Milligan, J. A. Aguilera, T-T. D. Nguyen, R. A. Paglinawan and J. F. Ward, DNA strand-break yields after post-irradiation incubation with base excision repair endonucleases implicate hydroxyl radical pairs in double-strand break formation. *Int. J. Radiat. Biol.* **76**, 1475–1483 (2000).
8. B. M. Sutherland, P. V. Bennett, O. Sidorkina and J. Laval, Clustered DNA damages induced in isolated DNA and in human cells by low doses of ionizing radiation. *Proc. Natl. Acad. Sci. USA* **97**, 103–108 (2000).
9. B. M. Sutherland, P. V. Bennett, O. Sidorkina and J. Laval, Clustered damages and total lesions induced in DNA by ionizing radiation: Oxidized bases and strand breaks. *Biochemistry* **39**, 8026–8031 (2000).
10. B. M. Sutherland, P. V. Bennett, O. Sidorkina and J. Laval, Clustered DNA damages induced by X rays in human cells. *Radiat. Res.* **157**, 611–616 (2002).
11. T. J. Jenner, J. Fulford and P. O'Neill, Contribution of base lesions to radiation-induced clustered DNA damage: Implication for models of radiation response. *Radiat. Res.* **156**, 590–593 (2001).
12. M. Gulston, J. Fulford, T. Jenner, C. de Lara and P. O'Neill, Clustered DNA damage induced by γ radiation in human fibroblasts (HF19), hamster (V79-4) cells and plasmid DNA is revealed as Fpg and Nth sensitive sites. *Nucleic Acids Res.* **30**, 3464–3472 (2002).

[2] A computer code implementing the Monte Carlo excision repair (MCER) model as well as results of sample calculations are available at http://rh.healthsciences.purdue.edu/mcer/.

13. A. Yokoya, S. M. Cunniffe and P. O'Neill, Effect of hydration on the induction of strand breaks and base lesions in plasmid DNA films by γ-radiation. *J. Am. Chem. Soc.* **124**, 8859–8866 (2002).
14. J. F. Ward, W. F. Blakely and E. I. Joner, Mammalian cells are not killed by DNA single-strand breaks caused by hydroxyl radicals from hydrogen peroxide. *Radiat. Res.* **103**, 383–392 (1985).
15. J. F. Ward, Radiation mutagenesis: The initial DNA lesions responsible. *Radiat. Res.* **142**, 362–368 (1995); Errata, *Radiat. Res.* **143**, 355 (1995).
16. S. Malyarchuk, R. Youngblood, A. M. Landry, E. Quillin and L. Harrison, The mutation frequency of 8-oxo-7,8-dihydroguanine (8-oxodG) situated in a multiply damaged site: Comparison of a single and two closely opposed 8-oxodG in Escherichia coli. *DNA Repair* **2**, 695–705 (2003).
17. C. G. Pearson, N. Shikazono, J. Thacker and P. O'Neill, Enhanced mutagenic potential of 8-oxo-7,8-dihydroguanine when present within a clustered DNA damage site. *Nucleic Acids Res.* **32**, 263–270 (2004).
18. M. Gulston, C. de Lara, T. Jenner, E. Davis and P. O'Neill, Processing of clustered DNA damage generates additional double-strand breaks in mammalian cells post-irradiation. *Nucleic Acids Res.* **32**, 1602–1609 (2004).
19. N. Yang, H. Galick and S. S. Wallace, Attempted base excision repair of ionizing radiation damage in human lymphoblastoid cells produces lethal and mutagenic double strand breaks. *DNA Repair* **3**, 1323–1334 (2004).
20. G. Dianov and T. Lindahl, Reconstitution of the DNA base excision-repair pathway. *Curr. Biol.* **4**, 1069–1076 (1994).
21. Y. Matsumoto, K. Kim and D. F. Bogenhagen, Proliferating cell nuclear antigen-dependent abasic site repair in *Xenopus laevis* oocytes: An alternative pathway of base excision DNA repair. *Mol. Cell. Biol.* **14**, 6187–6197 (1994).
22. G. Frosina, P. Fortini, O. Rossi, F. Carrozzino, G. Raspaglio, L. S. Cox, D. P. Lane, A. Abbondandolo and E. Dogliotti, Two pathways for base excision repair in mammalian cells. *J. Biol. Chem.* **271**, 9573–9578 (1996).
23. A. Klungland and T. Lindahl, Second pathway for completion of human DNA base excision-repair: Reconstitution with purified proteins and requirement for DNase IV (FEN1). *EMBO J.* **16**, 3341–3348 (1997).
24. H. Nilsen and H. E. Krokan, Base excision repair in a network of defence and tolerance. *Carcinogenesis* **22**, 987–998 (2001).
25. A. Memisoglu and L. Samson, Base excision repair in yeast and mammals. *Mutat. Res.* **451**, 39–51 (2000).
26. A. Sancar, DNA excision repair. *Annu. Rev. Biochem.* **65**, 43–81 (1996); Errata, *Annu. Rev. Biochem.* **66**, VII (1997).
27. R. D. Wood, Nucleotide excision repair in mammalian cells. *J. Biol. Chem.* **272**, 23465–23468 (1997).
28. J. J. Lin and A. Sancar, A new mechanism for repairing oxidative damage to DNA: (A)BC excinuclease removes AP sites and thymine glycols from DNA. *Biochemistry* **28**, 7979–7984 (1989).
29. Y. W. Kow, S. S. Wallace and B. Van Houten, UvrABC nuclease complex repairs thymine glycol, an oxidative DNA base damage. *Mutat. Res.* **235**, 147–156 (1990).
30. A. D. Scott, M. Neishabury, D. H. Jones, S. H. Reed, S. Boiteux and R. Waters, Spontaneous mutation, oxidative DNA damage, and the roles of base and nucleotide excision repair in the yeast *Saccharomyces cerevisiae*. *Yeast* **15**, 205–218 (1999).
31. C. A. Torres-Ramos, R. E. Johnson, L. Prakash and S. Prakash, Evidence for the involvement of nucleotide excision repair in the removal of abasic sites in yeast. *Mol. Cell. Biol.* **20**, 3522–3528 (2000).
32. J. C. Huang, D. S. Hsu, A. Kazantsev and A. Sancar, Substrate spectrum of human excinuclease: Repair of abasic sites, methylated bases, mismatches, and bulky adducts. *Proc. Natl. Acad. Sci. USA* **91**, 12213–12217 (1994).
33. J. T. Reardon, T. Bessho, H. C. Kung, P. H. Bolton and A. Sancar, *In vitro* repair of oxidative DNA damage by human nucleotide excision repair system: Possible explanation for neurodegeneration in

Xeroderma pigmentosum patients. *Proc. Natl. Acad. Sci. USA* **94**, 9463–9468 (1997).

34. P. J. Brooks, D. S. Wise, D. A. Berry, J. V. Kosmoski, M. J. Smerdon, R. L. Somers, H. Mackie, A. Y. Spoonde, E. J. Ackerman and J. H. Robbins, The oxidative DNA lesion 8,5′-(*S*)-cyclo-2′-deoxyadenosine is repaired by the nucleotide excision repair pathway and blocks gene expression in mammalian cells. *J. Biol. Chem.* **275**, 22355–22362 (2000).

35. I. Kuraoka, C. Bender, A. Romieu, J. Cadet, R. D. Wood and T. Lindahl, Removal of oxygen free-radical-induced 5′,8-purine cyclodeoxynucleosides from DNA by the nucleotide excision-repair pathway in human cells. *Proc. Natl. Acad. Sci. USA* **97**, 3832–3837 (2000).

36. S. S. Wallace, Enzymatic processing of radiation-induced free radical damage in DNA. *Radiat. Res.* **150** (Suppl.), S60–S79 (1998).

37. B. A. Sokhansanj, G. R. Rodrigue, J. P. Fitch and D. M. Wilson, III, A quantitative model of human DNA base excision repair. I. Mechanistic insights. *Nucleic Acids Res.* **30**, 1817–1825 (2002).

38. V. A. Semenenko and R. D. Stewart, Monte Carlo simulation of base and nucleotide excision repair of clustered DNA damage sites. II. Comparisons of model predictions to measured data. *Radiat. Res.* **164**, 194–201 (2005).

39. S. L. Wolfe, *Molecular and Cellular Biology*, p. 528. Wadsworth Publishing Company, Belmont, CA, 1993.

40. W. R. Holley and A. Chatterjee, Clusters of DNA damage induced by ionizing radiation: Formation of short DNA fragments. I. Theoretical modeling. *Radiat. Res.* **145**, 188–199 (1996).

41. B. Rydberg, Clusters of DNA damage induced by ionizing radiation: Formation of short DNA fragments. II. Experimental detection. *Radiat. Res.* **145**, 200–209 (1996).

42. R. Hanai, M. Yazu and K. Hieda, On the experimental distinction between ssbs and dsbs in circular DNA. *Int. J. Radiat. Biol.* **73**, 475–479 (1998).

43. H. Nikjoo, P. O'Neill, W. E. Wilson and D. T. Goodhead, Computational approach for determining the spectrum of DNA damage induced by ionizing radiation. *Radiat. Res.* **156**, 577–583 (2001).

44. V. V. Moiseenko, R. N. Hamm, A. J. Waker and W. V. Prestwich, The cellular environment in computer simulations of radiation-induced damage to DNA. *Radiat. Environ. Biophys.* **37**, 167–172 (1998).

45. W. Friedland, P. Jacob, H. G. Paretzke, M. Merzagora and A. Ottolenghi, Simulation of DNA fragment distributions after irradiation with photons. *Radiat. Environ. Biophys.* **38**, 39–47 (1999).

46. I. Mellon, G. Spivak and P. C. Hanawalt, Selective removal of transcription-blocking DNA damage from the transcribed strand of the mammalian DHFR gene. *Cell* **51**, 241–249 (1987).

47. P. K. Cooper, T. Nouspikel, S. G. Clarkson and S. A. Leadon, Defective transcription-coupled repair of oxidative base damage in Cockayne syndrome patients from XP group G. *Science* **275**, 990–993 (1997).

48. B. Pascucci, M. Stucki, Z. O. Jónsson, E. Dogliotti and U. Hübscher, Long patch base excision repair with purified human proteins. DNA ligase I as patch size mediator for DNA polymerases δ and ε. *J. Biol. Chem.* **274**, 33696–33702 (1999).

49. Y. Matsumoto, K. Kim, J. Hurwitz, R. Gary, D. S. Levin, A. E. Tomkinson and M. S. Park, Reconstitution of proliferating cell nuclear antigen-dependent repair of apurinic/apyrimidinic sites with purified human proteins. *J. Biol. Chem.* **274**, 33703–33708 (1999).

50. M. Weinfeld, A. Rasouli-Nia, M. A. Chaudhry and R. A. Britten, Response of base excision repair enzymes to complex DNA lesions. *Radiat. Res.* **156**, 584–589 (2001).

51. M. E. Lomax, M. K. Gulston and P. O'Neill, Chemical aspects of clustered DNA damage induction by ionising radiation. *Radiat. Prot. Dosim.* **99**, 63–68 (2002).

52. M. H. David-Cordonnier, S. Boiteux and P. O'Neill, Excision of 8-oxoguanine within clustered damage by the yeast OGG1 protein. *Nucleic Acids Res.* **29**, 1107–1113 (2001).

53. M. H. David-Cordonnier, J. Laval and P. O'Neill, Recognition and kinetics for excision of a base lesion within clustered DNA damage by the *Escherichia coli* proteins Fpg and Nth. *Biochemistry* **40**, 5738–5746 (2001).

54. M. H. David-Cordonnier, S. Boiteux and P. O'Neill, Efficiency of excision of 8-oxo-guanine within DNA clustered damage by XRS5 nuclear extracts and purified human OGG1 protein. *Biochemistry* **40**, 11811–11818 (2001).

55. M. H. David-Cordonnier, S. M. Cunniffe, I. D. Hickson and P. O'Neill, Efficiency of incision of an AP site within clustered DNA damage by the major human AP endonuclease. *Biochemistry* **41**, 634–642 (2002).

56. J. O. Blaisdell, L. Harrison and S. S. Wallace, Base excision repair processing of radiation-induced clustered DNA lesions. *Radiat. Prot. Dosim.* **97**, 25–31 (2001).

57. W. A. Beard and S. H. Wilson, Structural insights into DNA polymerase β fidelity: Hold tight if you want it right. *Chem. Biol.* **5**, R7–R13 (1998).

58. R. W. Sobol, J. K. Horton, R. Kühn, H. Gu, R. K. Singhal, R. Prasad, K. Rajewsky and S. H. Wilson, Requirement of mammalian DNA polymerase-β in base-excision repair. *Nature* **379**, 183–186 (1996); Errata, *Nature* **379**, 848 (1996); *Nature* **383**, 457 (1996).

59. P. Fortini, B. Pascucci, E. Parlanti, R. W. Sobol, S. H. Wilson and E. Dogliotti, Different DNA polymerases are involved in the short- and long-patch base excision repair in mammalian cells. *Biochemistry* **37**, 3575–3580 (1998).

60. M. Stucki, B. Pascucci, E. Parlanti, P. Fortini, S. H. Wilson, U. Hübscher and E. Dogliotti, Mammalian base excision repair by DNA polymerases δ and ε. *Oncogene* **17**, 835–843 (1998).

61. M. K. Shivji, V. N. Podust, U. Hübscher and R. D. Wood, Nucleotide excision repair DNA synthesis by DNA polymerase ε in the presence of PCNA, RFC, and RPA. *Biochemistry* **34**, 5011–5017 (1995).

62. J. Ahn, V. S. Kraynov, X. Zhong, B. G. Werneburg and M. D. Tsai, DNA polymerase β: Effects of gapped DNA substrates on dNTP specificity, fidelity, processivity and conformational changes. *Biochem. J.* **331**, 79–87 (1998).

63. W. P. Osheroff, H. K. Jung, W. A. Beard, S. H. Wilson and T. A. Kunkel, The fidelity of DNA polymerase β during distributive and processive DNA synthesis. *J. Biol. Chem.* **274**, 3642–3650 (1999).

64. A. M. Chagovetz, J. B. Sweasy and B. D. Preston, Increased activity and fidelity of DNA polymerase β on single-nucleotide gapped DNA. *J. Biol. Chem.* **272**, 27501–27504 (1997).

65. D. C. Thomas, J. D. Roberts, R. D. Sabatino, T. W. Myers, C. K. Tan, K. M. Downey, A. G. So, R. A. Bambara and T. A. Kunkel, Fidelity of mammalian DNA replication and replicative DNA polymerases. *Biochemistry* **30**, 11751–11759 (1991).

66. G. L. Dianov, P. O'Neill and D. T. Goodhead, Securing genome stability by orchestrating DNA repair: Removal of radiation-induced clustered lesions in DNA. *Bioessays* **23**, 745–749 (2001).

67. P. C. Hanawalt and G. Spivak, Transcription-coupled repair. Which lesions? Which diseases? In *Advances in DNA Damage and Repair* (M. Dizdaroglu and A. Karakaya, Eds.), pp. 169–179. Kluwer Academic/Plenum Publishers, New York, 1999.

68. G. L. Dianov, T. Thybo, I. I. Dianova, L. J. Lipinski and V. A. Bohr, Single nucleotide patch base excision repair is the major pathway for removal of thymine glycol from DNA in human cell extracts. *J. Biol. Chem.* **275**, 11809–11813 (2000).

69. P. Fortini, E. Parlanti, O. M. Sidorkina, J. Laval and E. Dogliotti, The type of DNA glycosylase determines the base excision repair pathway in mammalian cells. *J. Biol. Chem.* **274**, 15230–15236 (1999).

70. G. Dianov, A. Price and T. Lindahl, Generation of single-nucleotide repair patches following excision of uracil residues from DNA. *Mol. Cell. Biol.* **12**, 1605–1612 (1992).

71. K. Nealon, I. D. Nicholl and M. K. Kenny, Characterization of the DNA polymerase requirement of human base excision repair. *Nucleic Acids Res.* **24**, 3763–3770 (1996).

72. G. Dianov, C. Bischoff, J. Piotrowski and V. A. Bohr, Repair path-

ways for processing of 8-oxoguanine in DNA by mammalian cell extracts. *J. Biol. Chem.* **273**, 33811–33816 (1998).

*73.* Z. Lin and C. de los Santos, NMR characterization of clustered bistrand abasic site lesions: Effect of orientation on their solution structure. *J. Mol. Biol.* **308**, 341–352 (2001).

*74.* M. T. Hess, U. Schwitter, M. Petretta, B. Giese and H. Naegeli, Bipartite substrate discrimination by human nucleotide excision repair. *Proc. Natl. Acad. Sci. USA* **94**, 6664–6669 (1997).

*75.* S. Vispé and M. S. Satoh, DNA repair patch-mediated double strand DNA break formation in human cells. *J. Biol. Chem.* **275**, 27386–27392 (2000).

*76.* S. Vispé, E. L. Y. Ho, T. M. C. Yung and M. S. Satoh, Double-strand DNA break formation mediated by flap endonuclease-1. *J. Biol. Chem.* **278**, 35279–35285 (2003).

*77.* Z. Hatahet and S. S. Wallace, Translesion DNA synthesis. In *DNA Damage and Repair*, Vol. 1, *DNA Repair in Prokaryotes and Lower Eukaryotes* (J. A. Nickoloff and M. F. Hoekstra, Eds.), pp. 229–262. Humana Press, Totowa, NJ, 1998.

*78.* M. Purschke, U. Kasten-Pisula, I. Brammer and E. Dikomey, Human and rodent cell lines showing no differences in the induction but differing in the repair kinetics of radiation-induced DNA base damage. *Int. J. Radiat. Biol.* **80**, 29–38 (2004).

*79.* B. Kaina, DNA damage-triggered apoptosis: Critical role of DNA repair, double-strand breaks, cell proliferation and signaling. *Biochem. Pharmacol.* **66**, 1547–1554 (2003).

*80.* H. Budworth and G. L. Dianov, Mode of inhibition of short-patch base excision repair by thymine glycol within clustered DNA lesions. *J. Biol. Chem.* **278**, 9378–9381 (2003).

*81.* M. E. Lomax, S. Cunniffe and P. O'Neill, 8-OxoG retards the activity of the ligase III/XRCC1 complex during the repair of a single-strand break, when present within a clustered DNA damage site. *DNA Repair* **3**, 289–299 (2004).